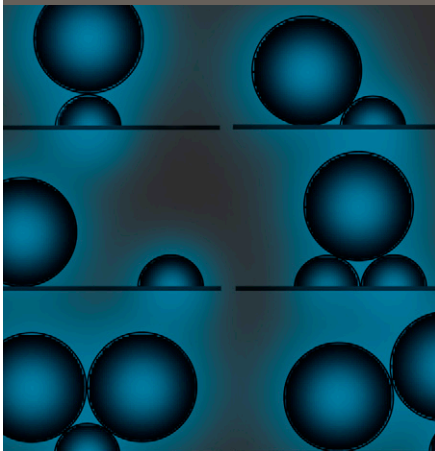


Chongyang Shen
Lian-Ping Wang
Baoguo Li
Yuanfang Huang*
Yan Jin*



Effects of surface roughness on detachment of colloids deposited at primary minima were examined via experiments and theoretical analysis. We provide theoretical demonstration and experimental evidence that colloids initially attached at tips of nanoscale protruding asperities will detach from a rough surface at low solution ionic strengths.

C. Shen, B. Li, and Y. Huang, Key Lab. of Plant-Soil Interactions, Ministry of Environment, Key Lab. of Soil and Water, Ministry of Agriculture, and Dep. of Soil and Water Sciences, China Agricultural Univ., Beijing 100193, China; L.-P. Wang, Dep. of Mechanic Engineering, Univ. of Delaware, Newark, DE 19716; and Y. Jin, Dep. of Plant and Soil Sciences, Univ. of Delaware, Newark, DE 19716. *Corresponding authors (yfhuang@china.com; yjin@udel.edu). Supplemental material is available online.

Vadose Zone J.
doi:10.2136/vzj2011.0057
Received 7 June 2011.

© Soil Science Society of America
5585 Guilford Rd., Madison, WI 53711 USA.
All rights reserved. No part of this periodical may be reproduced or transmitted in any form or by any means, electronic or mechanical, including photocopying, recording, or any information storage and retrieval system, without permission in writing from the publisher.

Role of Surface Roughness in Chemical Detachment of Colloids Deposited at Primary Energy Minima

This study theoretically and experimentally examined effects of surface roughness on detachment of colloids deposited under favorable chemical conditions on reduction of solution ionic strength. A superposition approach based on elemental geometric models was developed to estimate variation of Derjaguin–Landau–Verwey–Overbeek (DLVO) interaction energies between a colloid and a rough surface under different solution chemistries. Theoretical analysis showed that most colloids attached at rough surfaces via primary-minimum association are irreversible on reduction of solution ionic strength because primary minima are deeper and the detachment energy barriers are greater at lower ionic strength. A fraction of colloids initially attached at tips of nanoscale protruding asperities, however, will detach from a rough surface at low ionic strength because the net force acting on the colloids can become repulsive (i.e., calculated DLVO interaction energy curves show monotonic decreases of interaction energies with separation distance at low ionic strength). Column experiments were conducted with 1156-nm polystyrene latex particles and rough sand (300–355- μm diameter) to examine the detachment of colloids initially deposited at primary minima. Experimental results confirmed that a fraction of colloids are released at low ionic strengths. Our theoretical and experimental results are consistent with literature observations, adding convincing evidence to challenge the usual belief that colloids attached at primary minima are irreversible on reduction of solution ionic strength. Although the importance of surface heterogeneity on colloid deposition has been widely recognized, our study implies that surface heterogeneity also plays a critical role in colloid detachment under both favorable and unfavorable conditions.

Abbreviations: AFM, atomic force microscopy; DLVO, Derjaguin–Landau–Verwey–Overbeek; SEI, surface element integration.

Knowledge of colloid transport behavior in porous media is of importance in a variety of applications such as remediation of contaminated soil and groundwater, granular filtration in water and wastewater treatment, and natural filtration of pathogenic microorganisms (Ryan and Elimelech, 1996; Tufenkji and Elimelech, 2005; Shang et al., 2010). Deposition and detachment are two primary factors controlling the transport of colloids in porous media. Particle deposition in porous media has received considerable attention in the literature. In particular, a systematic framework, i.e., the colloid filtration theory (CFT) has been developed to predict particle deposition in porous media (Yao et al., 1971; Rajagopalan and Tien, 1976; Tufenkji and Elimelech, 2004a; Ma et al., 2009). The CFT considers that the colloid deposition rate is controlled by three individual mechanisms: Brownian diffusion, interception, and sedimentation. In CFT, the colloid deposition rate is characterized by single collector contact efficiency, a parameter that quantifies the frequency of colloid collisions with a collector grain. Despite successful predictions by the CFT for colloid deposition under favorable chemical conditions (i.e., when Derjaguin–Landau–Verwey–Overbeek [DLVO] interaction energy barriers are absent), large discrepancies have been frequently reported between theoretical calculations and experimental observations under unfavorable conditions (Ryan and Elimelech, 1996).

The CFT assumes that particle and collector surfaces are perfectly smooth; however, the surfaces of natural colloids and collectors all contain some degree of physical nonuniformity at various scales (Suresh and Walz, 1996). Therefore, surface roughness has been frequently regarded as one of the primary factors (surface roughness, charge heterogeneity, and secondary minimum) causing the discrepancies between theoretical predictions and experimental results (Elimelech and O'Melia, 1990a,b; Ryan and Elimelech, 1996;

Bhattacharjee et al., 1998; Cooper et al., 2001; Hoek et al., 2003; Hoek and Agarwal, 2006; Katainen et al., 2006; Shen et al., 2007, 2008; Jaiswal et al., 2009). Several mechanisms by which surface roughness influences colloid deposition have been disclosed. Of those, reduction of the DLVO interaction energies is considered the most significant according to theoretical analysis (Suresh and Walz, 1996; Bhattacharjee et al., 1998; Hoek et al., 2003; Hoek and Agarwal, 2006; Huang et al., 2010) and microscopic examinations (Bowen and Doneva, 2000; Suresh and Walz, 1997). In addition, Kempes and Bhattacharjee (2009) found that surface roughness could modify the flow field and increase the surface area available for colloid deposition. Sayers and Ryan (2005) demonstrated that surface roughness influences single collector contact efficiency.

The effect of surface roughness on colloid detachment has received much less attention in the literature. Colloid detachment occurs due to a disturbance to the hydrodynamics or solution chemistry in the system (Bergendahl and Grasso, 1999, 2000). In this study, these two types of detachments are referred to as *hydrodynamic detachment* and *chemical detachment*, respectively, following Das et al. (1994), Bergendahl and Grasso (1999, 2000), and Burdick et al. (2005). Das et al. (1994) and Burdick et al. (2005) investigated the effects of surface roughness on the hydrodynamic detachment of colloids and showed that surface roughness inhibits colloid detachment by increasing the dominance of adhesive torque over the hydrodynamic drag that colloids experience in the flow field. The influence of surface roughness on the chemical detachment of colloids from surfaces, however, remains unclear to date. Considerable studies (McDowell-Boyer, 1992; Ryan and Gschwend, 1994a,b; Roy and Dzombak, 1996; Bergendahl and Grasso, 1999; Canseco et al., 2009) indicated that the detachment of colloids due to chemical disturbance was caused by the variation of DLVO interaction energies between attached colloids and collector surfaces. Because surface roughness also influences DLVO interaction energies, it is reasonable to anticipate that surface roughness has important effects on chemical detachment of colloids.

This study theoretically investigated the role of surface roughness in the chemical detachment of colloids from surfaces using a modified Derjaguin approach. Special attention was paid to the detachment of colloids initially deposited under favorable chemical conditions. We selected this condition to eliminate the interference of secondary minimum energy so that the role of surface roughness could be examined more unambiguously. Our results showed that the responses of the attached colloids to chemical disturbance depend on local geometric configurations in the colloid–rough surface systems. Most colloids deposited under favorable chemical conditions are chemically irreversible; however, a fraction of colloids attached at the tip of nanoscale protruding asperities can be detached when low ionic strength (e.g., 0.001 mol L⁻¹ in this study) solutions are introduced. The theoretical findings were supported by column experiment results from the present study and additional observations reported in the literature (Ryan

and Gschwend, 1994a,b; Chen and Elimelech, 2006; Tosco et al., 2009; Hahn et al., 2004; Roy and Dzombak, 1996).

Theoretical Considerations

To quantify the influence of surface roughness on the DLVO interaction energies during the detachment process, accurate representation of the surface roughness is required; however, the geometric complexity of rough surfaces inhibits its rigorous description by any mathematical models (Hoek et al., 2003). In addition, because surface roughness varies from place to place even for one collector (e.g., Supplemental Fig. S1; supplemental material is available online), it is impractical to calculate DLVO interaction energies at all locations for all collectors in a porous medium. To surmount this obstacle, an alternative is to introduce elementary models of a rough surface and examine their effects on DLVO interaction energies. Atomic force microscopy (AFM) images (Suresh and Walz, 1997; Bowen and Doneva, 2000; Rabinovich et al., 2000; Hoek et al., 2003; Katainen et al., 2006; Jaiswal et al., 2009; Shen et al., 2011) showed that rough surfaces consist of two main components: convex asperities and concave valleys between the asperities. In this study, we considered the interaction of a sphere with either one hemisphere on a flat surface or with two hemispheres against each other (see Fig. 1a and 1d) to represent the aforementioned two rough components. Treating a rough surface as a smooth plate covered with hemispheres has been used in a number of previous studies (Suresh and Walz, 1996; Bhattacharjee et al., 1998; Hoek et al., 2003; Hoek and Agarwal, 2006). Figures 1a to 1d schematically present typical stable deposition morphologies for the interaction of a colloid with the two rough configurations. The attachments in these scenarios are stable because the applied and adhesive forces and torques that the colloid experiences at these locations can be balanced. To calculate

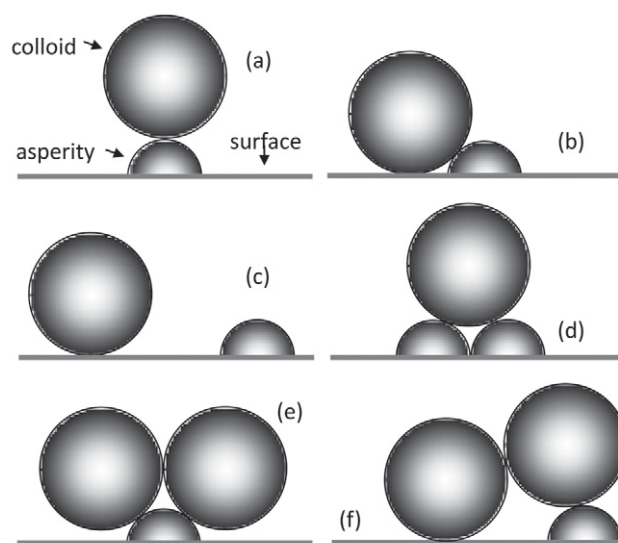


Fig. 1. Schematics of interactions of colloids with smooth surfaces covered with hemispheres.

the variation of DLVO interaction energy profiles with chemical disturbance for these interaction configurations, we assumed that the colloid leaves the rough surface along a line perpendicular to the flat surface.

Surface element integration (SEI) has been developed to calculate the effects of surface roughness on DLVO interaction energies. The SEI calculates DLVO interaction energies by integration of the interaction energy of elements with elements using the exact geometry of the rough surfaces. For each element–element interaction, the result of the interaction energy between two infinite flat plates is used (Bhattacharjee et al., 1998). This approach only considers the interactions with the rough surface area that overlaps with the projected area of the approaching colloid (Bhattacharjee et al., 1998; Huang et al., 2010). Therefore, it is not suitable for calculating the interactions of colloids with concave surfaces (e.g., Fig. 1b) where sidewall interactions (i.e., colloid–asperity interactions in Fig. 1b) are significant. Similar to previous studies (Elimelech and O’Melia, 1990a,b; Hoek et al., 2003; Shen et al., 2008, 2011), the effects of surface roughness in this study were determined as the sum of particle–surface (sphere–plate) and particle–asperity (sphere–sphere) DLVO interaction energies. The retarded van der Waals attraction (Φ^{vdW}) energies for colloid–asperity (pg) interaction and colloid–flat surface (ps) interaction were calculated as (Ho and Higuchi, 1968)

$$\begin{aligned}\Phi_{\text{pg}}^{\text{vdW}}(b) &= -\frac{Aa_g a_p}{6(a_p + a_g)b} \left(\frac{1}{1 + 11.12b/\lambda} \right) \\ \Phi_{\text{ps}}^{\text{vdW}}(H) &= -\frac{Aa_p}{6H} \left(\frac{1}{1 + 11.12H/\lambda} \right)\end{aligned}\quad [1]$$

where A is the Hamaker constant, a_g is the asperity radius, a_p is the colloid radius, b is the separation distance (surface to surface) between a colloid and an asperity, H is the separation distance between a colloid and a flat surface, and λ is a characteristic wavelength of the dielectric, usually taken as 100 nm (Hahn and O’Melia, 2004; Hahn et al., 2004). The electrical double layer potentials (Φ^{dl}) of colloid–asperity and colloid–flat surface interactions for constant surface potentials were calculated as (Hogg et al., 1966)

$$\begin{aligned}\Phi_{\text{pg}}^{\text{dl}}(b) &= \frac{\pi\epsilon\epsilon_0 a_g a_p}{a_g + a_p} \left\{ 2\psi_p \psi_g \ln \left[\frac{1 + \exp(-\kappa b)}{1 - \exp(-\kappa b)} \right] \right. \\ &\quad \left. + (\psi_p^2 + \psi_g^2) \ln [1 - \exp(-2\kappa b)] \right\}\end{aligned}\quad [2a]$$

$$\begin{aligned}\Phi_{\text{ps}}^{\text{dl}}(H) &= \pi\epsilon\epsilon_0 a_p \left\{ 2\psi_p \psi_s \ln \left[\frac{1 + \exp(-\kappa H)}{1 - \exp(-\kappa H)} \right] \right. \\ &\quad \left. + (\psi_p^2 + \psi_s^2) \ln [1 - \exp(-2\kappa H)] \right\}\end{aligned}\quad [2b]$$

where ϵ_0 is the permittivity of a vacuum, ϵ is the relative water dielectric constant or relative permittivity of water, κ is the reciprocal double layer thickness, and ψ_p , ψ_g , and ψ_s are the zeta potentials of the colloid, asperity, and surface, respectively. We assume $\psi_g = \psi_s$.

When the extended DLVO approach is considered, the short-range repulsion (e.g., hydration) has to be included, which can be evaluated by calculating the Born potential energy (Ryan and Elimelech, 1996). Feke et al. (1984) developed an equation to calculate the Born potential (Φ^{Born}) for sphere–sphere interaction:

$$\begin{aligned}\Phi_{\text{pg}}^{\text{Born}}(b) &= \frac{A}{37800R} \left(\frac{\sigma}{a_p} \right)^6 \\ &\quad \times \left[\frac{-R^2 - 7(x-1)R - 6(x^2 - 7x + 1)}{(R-1+x)^7} \right. \\ &\quad \left. + \frac{-R^2 + 7(x-1)R - 6(x^2 - 7x + 1)}{(R+1-x)^7} \right. \\ &\quad \left. + \frac{R^2 + 7(x+1)R + 6(x^2 + 7x + 1)}{(R+1+x)^7} \right. \\ &\quad \left. + \frac{R^2 - 7(x+1)R + 6(x^2 + 7x + 1)}{(R-1-x)^7} \right]\end{aligned}\quad [3]$$

where $x = a_g/a_p$, $R = 1 + x + b/a_p$ is the center-to-center separation distance normalized by a_p , and σ is the collision parameter. A typical, experimentally derived value for σ is 0.5 nm (Ruckenstein and Prieve, 1976; Feke et al., 1984; Hahn et al., 2004). The expression to calculate the Born potential for sphere–plane interaction can be written as (Ruckenstein and Prieve, 1976)

$$\Phi_{\text{ps}}^{\text{Born}}(H) = \frac{A\sigma^6}{7560} \left[\frac{8a_p + H}{(2a_p + H)^7} + \frac{6a_p - H}{H^7} \right]\quad [4]$$

The total extended DLVO interaction energies (Φ_{T}) for the configurations of Fig. 1a, 1b, 1d, and 1e were calculated using the equations shown in Table 1, which were obtained based on the following superposition. For example, take the case of Fig. 1d. The colloid particle interacts with two hemisphere asperities and a flat surface, therefore,

$$\begin{aligned}\Phi_{\text{T}} &= 2 \left[\Phi_{\text{pg}}^{\text{vdW}}(b) + \Phi_{\text{pg}}^{\text{dl}}(b) + \Phi_{\text{pg}}^{\text{Born}}(b) \right] \\ &\quad + \left[\Phi_{\text{ps}}^{\text{vdW}}(H) + \Phi_{\text{ps}}^{\text{dl}}(H) + \Phi_{\text{ps}}^{\text{Born}}(H) \right] \\ &\equiv 2\Phi_{\text{pg}}(b) + \Phi_{\text{ps}}(H)\end{aligned}\quad [5]$$

Table 1. The equations used to calculate total extended DLVO interaction energies (Φ_T) for the four typical cases shown in Fig. 1.

Scenario	Calculation equations†
Case 1 of Fig. 1a	$\Phi_T = \Phi_{pg}(h) + \Phi_{ps}(h + a_g)$
Case 2 of Fig. 1b	$\Phi_T = \Phi_{pg}(h) + \Phi_{ps}\left[\sqrt{(b + a_p)^2 + 2ba_g} - a_p\right]$
Case 3 of Fig. 1d	$\Phi_T = 2\Phi_{pg}(h) + \Phi_{ps}\left[\sqrt{(b + a_p + a_g)^2 - a_g^2} - a_p\right]$
Case 4 of Fig. 1e	$\Phi_T = 2\Phi_{pg}(h) + 2\Phi_{ps}\left[\sqrt{(a_p + a_g + b)^2 - a_p^2} - a_p\right]$ at $a_g > (\sqrt{2}-1)a_p$ $\Phi_T = 2\Phi_{ps}(H) + 2\Phi_{pg}\left[\sqrt{(a_p + H)^2 + a_p^2} - a_p - a_g\right]$ at $a_g \leq (\sqrt{2}-1)a_p$

† Φ_{pg} , DLVO interaction energy between a colloid and an asperity; Φ_{ps} , DLVO interaction energy between a colloid and a flat surface; h , surface-to-surface separation distance between a colloid and an asperity; H , surface-to-surface separation distance between a colloid and the reference flat surface; Φ_{pg} and Φ_{ps} are functions of the expressions in the parentheses and brackets.

where, in this case, if the colloid is located symmetrically above the two asperities (or detached from the flat surface perpendicularly), the geometric relation between h and H is

$$(H + a_p)^2 + a_g^2 = (h + a_p + a_g)^2 \quad [6]$$

In this simple superposition treatment, there is a certain level of repetition. When $a_g \ll a_p$, Eq. [5] recovers the correct limiting behavior because all terms for colloid–asperity interactions approach zero. When a_g and a_p are comparable, Eq. [5] can be viewed as a reasonable first approximation because the colloid–asperity interaction will dominate over the colloid–flat surface interactions for the case in Fig. 1d; in other words, the additional colloid–surface interactions that represent double counting are relatively small. A similar argument can be used to justify the superposition treatment as a first approximation for the cases shown in Fig. 1a, 1d, and 1e. For all the cases considered in Table 1, the colloid is assumed to be detached from the surface perpendicularly relative to the reference flat surface. Details for the derivation of the equations in Table 1 can be found in the Supplemental Material.

The interaction energy for the configuration of Fig. 1c is equal to that of the interaction of a colloid with a flat surface (i.e., $a_g = 0$ nm), namely, the asperity is too far to influence the deposition of the colloid.

Experimental Materials and Procedures

Colloidal Particles and Porous Media

White carboxyl-modified polystyrene latex microspheres (Interfacial Dynamics Corp., Portland, OR) with a diameter of 1156 nm were used as model colloids. They are hydrophilic, with a density of 1.055 g cm^{-3} (as reported by the manufacturer). Colloidal concentrations were determined by UV-Vis spectrophotometry (DU Series 640, Beckman Instruments, Fullerton, CA) at a 440-nm wavelength.

Quartz sand with a diameter ranging from 300 to 355 μm was used as the model collector grains. The sand was sieved from Accusand 40/60 (Unimin Corp., Le Sueur, MN) with a stainless steel mesh. The procedure of Zhuang et al. (2005) was used to elaborately remove metal oxides and other impurities from the sand and glass beads.

The electrophoretic mobilities of the colloids and sand in NaCl electrolyte solutions of different ionic strengths were determined by a Zetasizer Nano ZS (Malvern Instruments, Southborough, MA) at 25°C . The finest fraction of sand sieved from the Accusand was used for the measurement. The determined zeta potentials for the colloid were -27.38 , -35.21 , and -46.73 mV at 0.3, 0.2, and 0.001 mol L^{-1} ionic strengths, respectively. The zeta potentials for the sand were -20.37 , -27.49 , and -39.27 mV at 0.3, 0.2, and 0.001 mol L^{-1} ionic strengths, respectively. The 0.3 mol L^{-1} solution had a pH of 10 and the 0.2 and 0.001 mol L^{-1} solutions had pH values of 6.0 to 6.5.

The surface roughness of the sand was measured using a bioscope atomic force microscope (Veeco Instruments, Plainview, NY) mounted on an Axiovert 200 inverted fluorescent microscope (Carl Zeiss, Jena, Germany). Sand grains were bonded to glass microscope slides with epoxy and the surface roughness was then measured with contact-mode imaging in air using silicon tips of 8-nm radius curvature (Veeco Instruments).

Colloid Deposition and Detachment Experiments

Colloid transport experiments were conducted in acrylic columns packed with the sand. The column setup used in this study was similar to that used in Shen et al. (2007). Briefly, the column was 3.8 cm in diameter and 10 cm long, with a top and a bottom plate. The sand was wet-packed in deionized water with vibration to minimize layering and air entrapment in the column. The porosity of the packed bed for each experiment was determined to be 0.33 (based on a particle density of 2.65 g cm^{-3} for the sand).

The first set of experiments was conducted to examine the chemical reversibility of colloids deposited in NaCl electrolyte solutions. Analytical reagent-grade NaCl (Fisher Scientific, Pittsburgh, PA) and deionized water were used to prepare the electrolyte solutions at three ionic strengths (0.001, 0.2, and 0.3 mol L⁻¹). The pH of the electrolyte solutions was adjusted by addition of NaOH and NaHCO₃. The experiments were performed at a fixed approach velocity of 8.0 × 10⁵ m s⁻¹ to avoid hydrodynamic detachment. For each experiment, degassed NaCl electrolyte solution at 0.3 mol L⁻¹ and pH 10 was first delivered to the column upward for at least 20 pore volumes to standardize the ionic strength and pH of the system. Then a three-step procedure, similar to that adopted in the previous studies (Shen et al., 2007, 2008; Hahn and O'Melia, 2004), was used for colloid deposition and release. Briefly, six pore volumes of colloid suspension (10 mg L⁻¹, corresponding to 1.2 × 10¹⁰ particles L⁻¹) in 0.3 mol L⁻¹ NaCl at pH 10 were first introduced to the packed column (Phase 1), followed by elution with colloid-free electrolyte solution of the same ionic strength and pH (Phase 2), and finally with electrolyte solutions at 0.2 or 0.001 mol L⁻¹ at pH 6.0 to 6.5 until no colloids were detected in the effluent (Phase 3).

The second set of column transport experiments was to examine the chemical reversibility of colloids deposited in CaCl₂ electrolyte solutions. For each experiment, the three-step procedure presented above was used to quantify colloid deposition and release. The ionic strength of the CaCl₂ electrolyte solutions used in Phases 1 and 2 was 0.2 mol L⁻¹ and in Phase 3 was 0.1 or 0.001 mol L⁻¹. The pH of the electrolyte solutions used in Phases 1 and 2 was 6.0 to 6.5 and in Phase 3 was 5.2.

Results

DLVO Interaction Energy Curves

The DLVO theory was used to infer whether detachment can occur for colloids deposited in the presence of surface roughness at 0.3 mol L⁻¹ NaCl on elution with NaCl electrolyte solutions at 0.2 or 0.001 mol L⁻¹ ionic strength. The measured zeta potentials of the colloid and sand in NaCl electrolyte solutions were adopted for theoretical calculations. A value of 1 × 10²⁰ J was chosen as the Hamaker constant for the polystyrene–water–quartz system (Elimelech and O'Melia, 1990a,b; Shen et al., 2007, 2008, 2010).

Because an atomic force microscope image showed that the height and curvature of the asperities on the

sand surface varied significantly (see Supplemental Fig. S1), we considered the interaction of colloids with rough surfaces with a wide range of asperity radii (0–5000 nm) in the theoretical calculations. Figure 2 presents DLVO energy profiles for the interaction

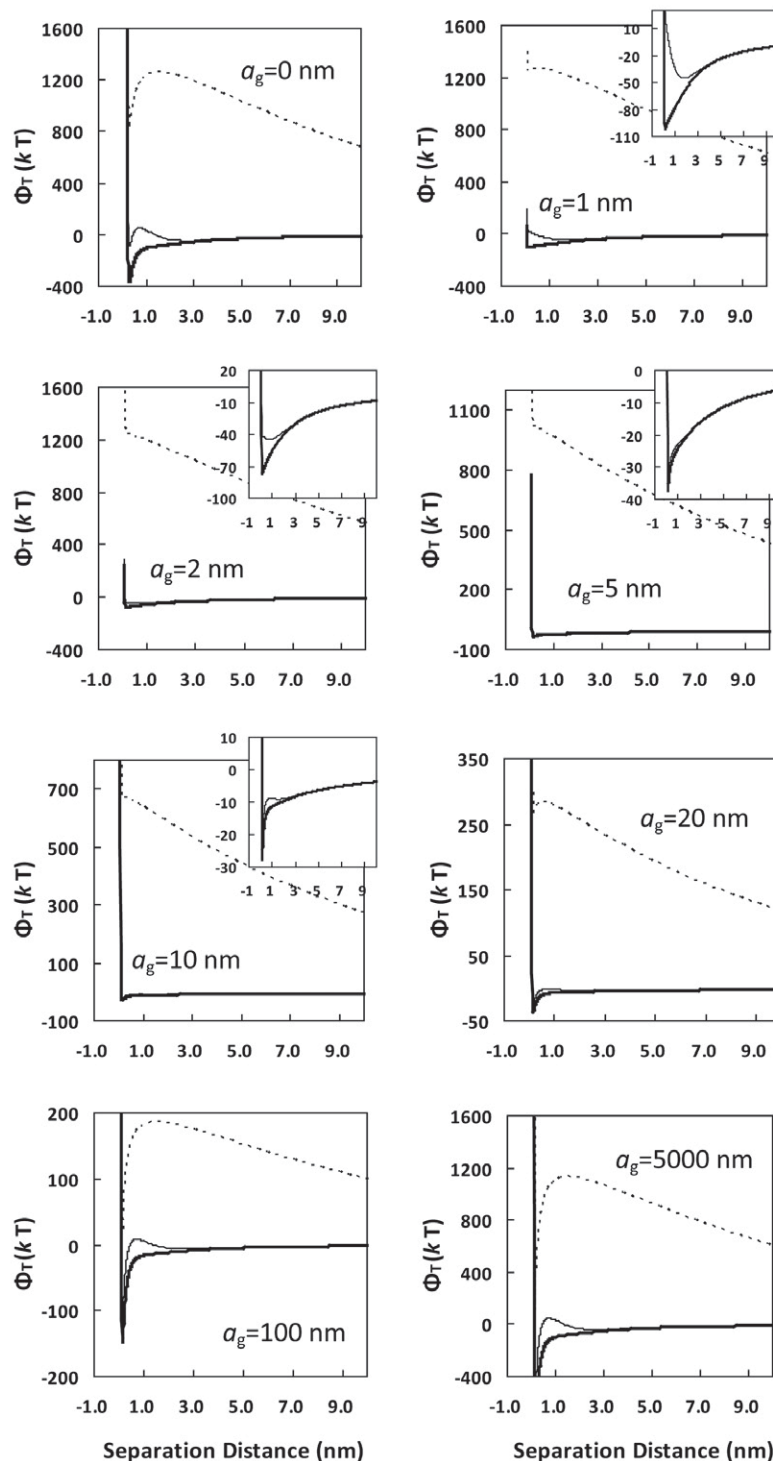


Fig. 2. The DLVO interaction energy (Φ_T) profiles for the rough configuration in Fig. 1a with different asperity radii (a_g) at different ionic strengths (thick solid line, 0.3 mol L⁻¹; thin solid line, 0.2 mol L⁻¹; dashed line, 0.001 mol L⁻¹). Note the change in scale of the y axes among the various graphs. Inserts are replotted figures at a different y axis scale to highlight the primary minimum.

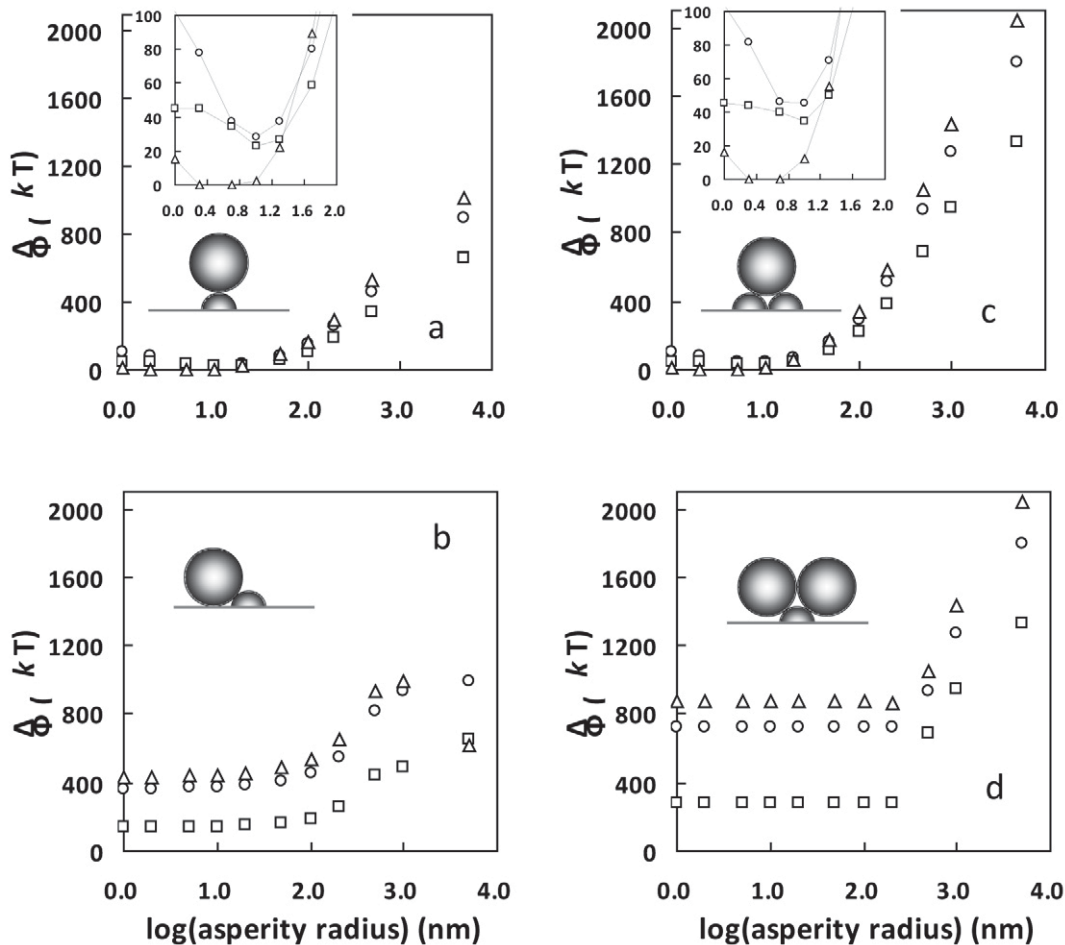


Fig. 3. Calculated detachment energy barrier ($\Delta\Phi$) for different colloid-rough surface configurations as a function of the asperity radius at different ionic strengths (triangle, 0.001 mol L⁻¹; square, 0.2 mol L⁻¹; circle, 0.3 mol L⁻¹). The values of $\Delta\Phi$ were obtained by subtracting the primary minimum from the maximum energy barrier under unfavorable conditions or equating them to primary minimum depths under favorable conditions or zero when the primary minimum and energy barrier disappear. Inserts are the corresponding interaction configurations and replotted figures at a different y axis scale.

configuration shown in Fig. 1a at 0.3, 0.2, and 0.001 mol L⁻¹ ionic strengths. At 0.3 mol L⁻¹, only primary minima exist in the DLVO energy profiles for all asperity radii considered; therefore, all colloids are deposited at primary minima. For $a_g = 0$ nm and $a_g > 10$ nm, when the solution ionic strength is reduced to 0.2 mol L⁻¹, steeper increases of potential energies (representing a stronger attractive force) from the separation distance corresponding to the primary minimum are obtained. This indicates that, for these sizes, the colloids initially deposited in primary minima at 0.3 mol L⁻¹ are irreversible in these cases. Although primary minima are shallower at 0.2 mol L⁻¹ than at 0.3 mol L⁻¹ for $1 \text{ nm} \leq a_g \leq 10$ nm, colloid release is still difficult because these conditions are favorable for colloid deposition (i.e., no repulsive force exists at the separation distance corresponding to the primary minimum where the colloids are located). To further understand whether detachment happens at 0.2 mol L⁻¹, the values of the detachment energy barrier ($\Delta\Phi$) were calculated by subtracting the primary minimum from the maximum energy barrier under unfavorable conditions

or equating it to the primary minimum depth under favorable conditions (see Fig. 3). Colloids retained in primary minima have to overcome the detachment energy barrier to successfully release back into bulk solutions. Figure 3a shows that detachment energy barriers are lower at 0.2 mol L⁻¹ than at 0.3 mol L⁻¹ for all asperity radii; however, even the smallest detachment energy barrier (22.56 kT , where k is the Boltzmann constant and T is the absolute temperature) at 0.2 mol L⁻¹ is still much larger than the average Brownian kinetic energy (1.5 kT). In addition, the calculated adhesive torque is much larger than the hydrodynamic torque (see Shen et al., 2010). Therefore, no detachment is expected at 0.2 mol L⁻¹ for the interaction configuration shown in Fig. 1a. When the solution ionic strength is decreased from 0.3 to 0.001 mol L⁻¹, steeper increases of potential energies with separation distance from the primary minima are obtained for $a_g < 2$ nm and $a_g > 10$ nm (see Fig. 3). Consequently, the deposited colloids are irreversible at 0.001 mol L⁻¹ under these conditions. For $2 \text{ nm} \leq a_g \leq 10$ nm, however, monotonic decreases in the interaction energies with

increasing separation distance are found at 0.001 mol L^{-1} . This indicates that colloids experience repulsive forces, and the colloids deposited in primary minima at 0.3 mol L^{-1} will be released at 0.001 mol L^{-1} in these cases.

It is interesting to note that traditionally the DLVO interaction energy curve is characterized by a deep attractive well (the primary minimum) at a small separation distance, a maximum energy barrier, and a shallow attractive well (the secondary minimum) at larger distances under unfavorable conditions. Both energy barrier and secondary minimum disappear and only the primary minimum exists in the DLVO interaction energy curves under favorable conditions. Our study, however, provides a new type of DLVO interaction energy curve under unfavorable conditions, that is, the interaction energy decreases monotonically with increasing separation distance due to the influence of surface roughness. Figures 4a to 4c schematically illustrate how the asperity size affects the interaction forces between an attached colloid and the rough configuration in Fig. 1a at 0.001 mol L^{-1} . Figure 4a shows that when the asperity is very small (e.g., $< 2 \text{ nm}$), the colloid is at the deep primary minimum of the energy curve for the colloid–flat surface interaction. Therefore, both the flat surface and the asperity attract the colloid. When the asperity radius is between 2 and 10 nm (Fig. 4b), the colloid experiences a strong repulsion from the bottom flat surface, and the primary minimum of the energy curve for the colloid–asperity interaction is relatively small and as such is eliminated by the strong repulsion from the bottom flat surface. Therefore, the primary minimum disappears in these cases and the colloid will be released back into the bulk solution due to the strong repulsion. When the asperity radius is further increased (e.g., $> 20 \text{ nm}$; see Fig. 4c), the colloid only experiences weak repulsion from the bottom flat surface due to the greater separation distance, and at the same time the attraction between the colloid and asperity gains strength to play a dominant role, resulting in a net attraction. At the ionic strength of 0.2 mol L^{-1} , the colloid is at the primary minimum and the secondary minimum of the energy profile for the colloid–flat surface interaction for $a_g < 1 \text{ nm}$ and $a_g > 2 \text{ nm}$, respectively. At $1 \text{ nm} \leq a_g \leq 2 \text{ nm}$, the attraction between the colloid and the asperity exceeds the repulsion from the bottom flat surface. Therefore, no monotonic decrease of interaction energy is observed at 0.2 mol L^{-1} .

Figure 5 presents representative DLVO energy profiles for the interaction configuration shown in Fig. 1b at 0.3, 0.2, and 0.001 mol L^{-1} ionic strengths. No monotonic decreases of interaction energies were found for any asperity radii at 0.2 and 0.001 mol L^{-1} , and

significant detachment energy barriers exist in all these cases (see Fig. 3c). This is because, at small separations, the colloids always experience attractions from both the asperity and the flat surface because H is roughly equal to $(1 + a_g/a_p)b$. Consequently, no detachment is expected at either 0.2 or 0.001 mol L^{-1} for this interaction configuration. These results indicate that, even for a given roughness size, depending on where the colloid is located relative to the asperity (Fig. 1a vs. 1b), it experiences different DLVO interaction forces. The DLVO energy profiles obtained for the interaction configuration in Fig. 1d at 0.3, 0.2, and 0.001 mol L^{-1} ionic strengths (data not shown) are very similar to those for the interaction configuration in Fig. 1a, leading to the same

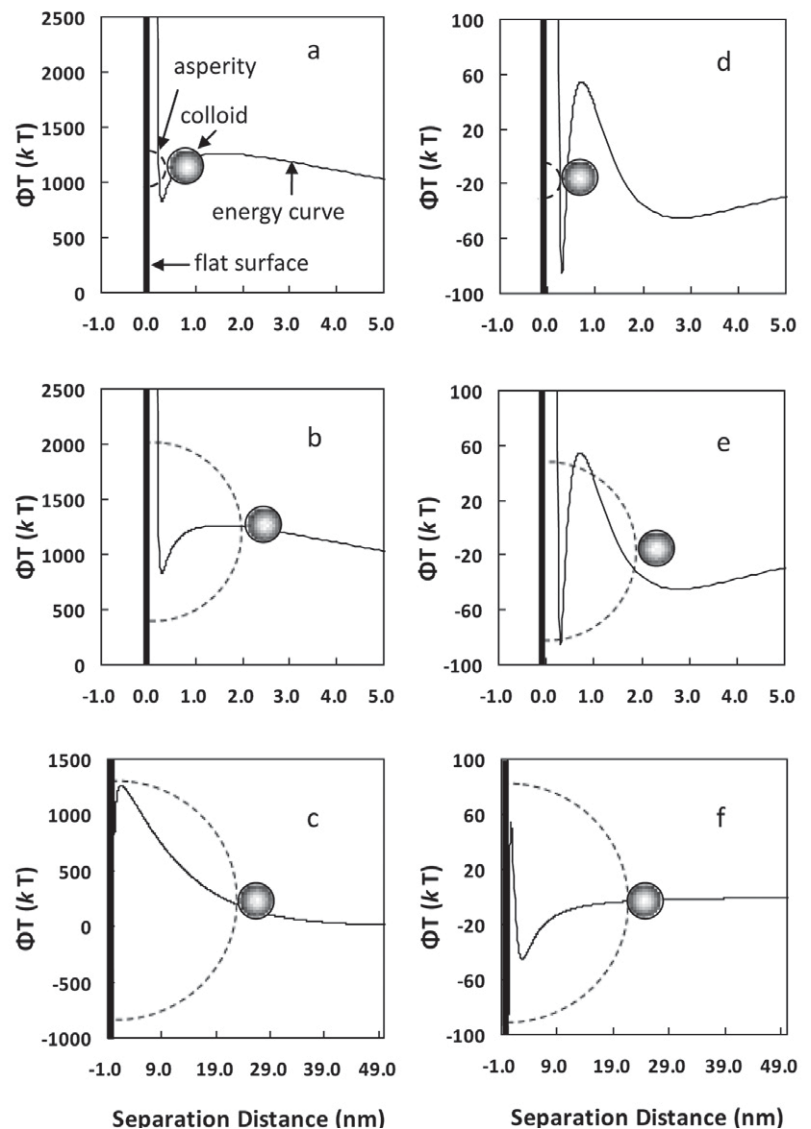


Fig. 4. Illustration of the effects of asperity size (a_g) on the interaction forces (Φ_T) between the 1156-nm colloid and rough surfaces at 0.001 mol L^{-1} for (a) $a_g < 2 \text{ nm}$, (b) $2 \text{ nm} \leq a_g \leq 10 \text{ nm}$, and (c) $a_g > 20 \text{ nm}$ and at 0.2 mol L^{-1} for (d) $a_g < 1 \text{ nm}$, (e) $1 \text{ nm} \leq a_g \leq 2 \text{ nm}$, and (f) $a_g > 2 \text{ nm}$. The curve shows the interaction energy profile between the colloid and the flat bottom surface. The interaction energy curve between the colloid and the asperity is not shown. Note the change in scale of the x and y axes among the various graphs and the reduced size of the colloid.

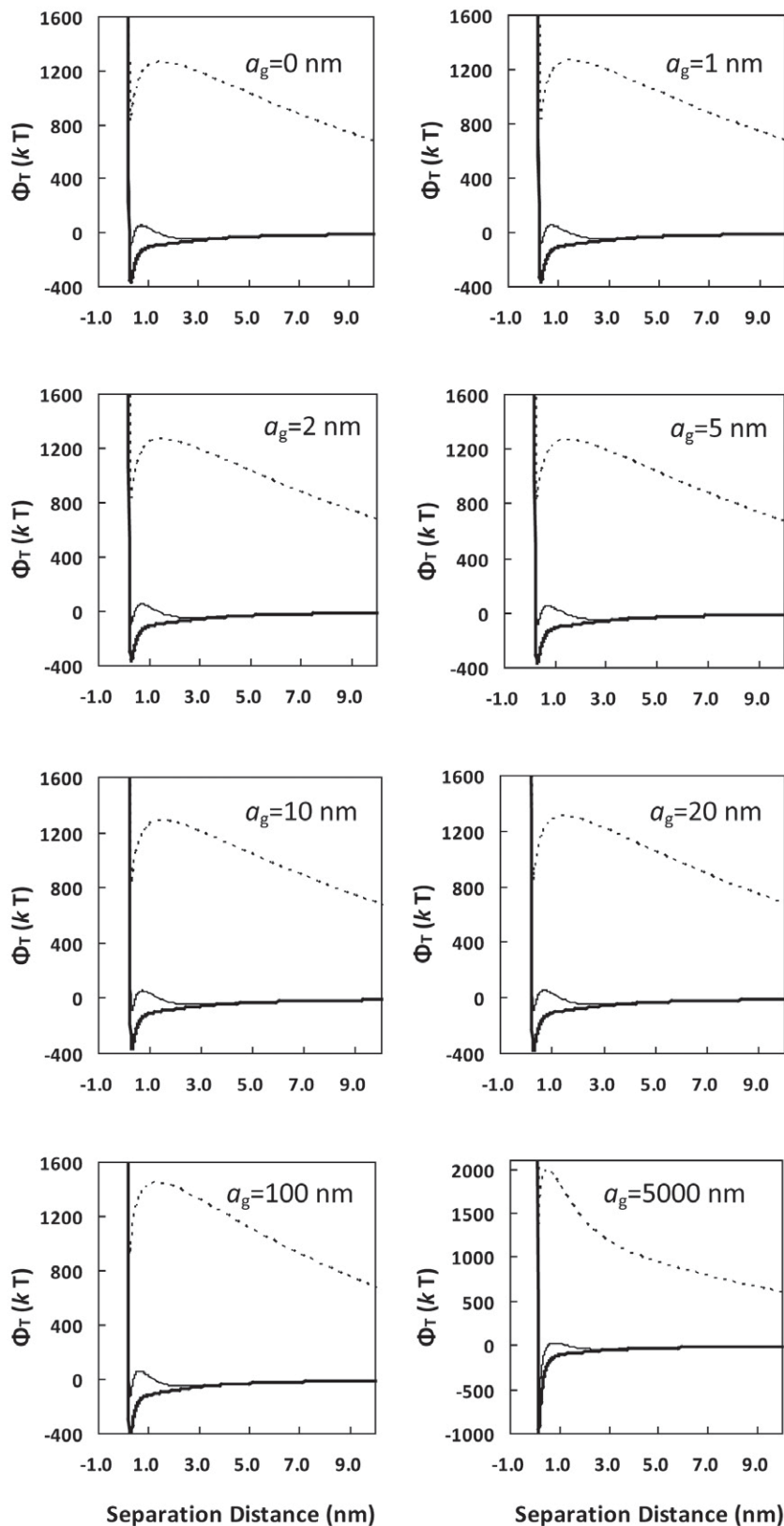


Fig. 5. The DLVO interaction energy (Φ_T) profiles for the rough configuration in Fig. 1b with different asperity radii (a_g) at different ionic strengths (thick solid line, 0.3 mol L^{-1} ; thin solid line, 0.2 mol L^{-1} ; dashed line, 0.001 mol L^{-1}). Note the change in scale of the y axes among the various graphs.

conclusions as above. Because colloids commonly aggregate under favorable conditions, the interaction of an aggregate (consisting of two colloids) with the convex surface was considered (Fig. 1e). As shown in Fig. 3, significant detachment energy barriers exist at 0.2 and 0.001 mol L^{-1} for all asperity radii in this case; therefore, aggregation inhibits colloid detachment (Fig. 2e vs. 2a).

In summary, colloids are deposited in primary minima in a NaCl electrolyte solution at 0.3 mol L^{-1} ionic strength for all cases considered (i.e., Fig. 1a, 1b, 1d, and 1e). When the solution ionic strength is reduced to 0.2 mol L^{-1} , no detachment is anticipated. When the solution ionic strength is reduced to 0.001 mol L^{-1} , most colloids remain trapped by the primary minima because a steeper local increase of potential energies and significant energy barriers are present. A small fraction of colloids at the tip of nanoscale protruding asperities will be released, however, due to the replacement of the primary energy minimum with a repulsive interaction caused by the insertion of the asperities between the colloid and the bottom flat surface. Similar theoretical results are obtained for the deposition and release of colloids in CaCl_2 electrolyte solution (data not shown). Although our calculations were based on elementary models of rough surfaces (i.e., Fig. 1), the observed variations in DLVO interaction energy curves with local geometric configurations of a rough surface are applicable to the local interactions of a colloid with a realistic rough surface in natural systems. Specifically, a monotonic decrease in interaction energies will occur provided that the primary minimum of the interaction between the colloid and the nearest asperity (not only hemispheric) can be eliminated by the repulsion from the bottom surface (not only flat). As shown below, the theoretical calculations are consistent with the experimental results obtained in the current study as well as those reported in the literature, indicating that our analysis provides meaningful insights into how surface roughness affects colloid detachment.

It is worth mentioning that we assumed constant surface potentials to calculate the double layer interaction energy (i.e., Eq. [2a–2b]). The calculated interaction energy barriers are lower than those from constant charge expression. Therefore, if constant surface charges are assumed, the monotonic decrease in interaction energies will be more significant.

Huang et al. (2010) demonstrated that the DLVO interaction energies calculated by SEI are similar to those calculated by

$$\Phi_T = f\Phi_{pg} + (1-f)\Phi_{ps} \quad [7]$$

where f is the fractional interaction between asperities and a colloid and $(1-f)$ is the fractional interaction between a flat surface and the colloid. Calculated DLVO energy profiles using Eq. [7] for the interaction configurations of Fig. 1a and 1d predict more detachments than the current results using the superposition approach. For example, monotonic decreases in interaction energies at zero separation distance were found at $2 \text{ nm} \leq a_g \leq 50 \text{ nm}$ and 0.001 mol L^{-1} for the interaction configuration of Fig. 1a (see Supplemental Fig. S2). This range of asperity radius is larger than that calculated using superposition (i.e., $2 \text{ nm} \leq a_g \leq 10 \text{ nm}$). Equation [7] and SEI are not appropriate for calculating the energy profile for the interaction configuration of Fig. 1b. In this case, the attractive interaction with the asperity on the side can be significant, as demonstrated above. Equation [7] and SEI, however, only consider the interactions with the rough surface area that overlaps with the projected area of the approaching colloid and tends to underestimate the interaction energy between the colloid and the asperity in this case.

Colloid Deposition and Release in Column Experiments

Figure 6 presents colloid breakthrough curves from the two deposition and release experiments in NaCl electrolyte solutions, where normalized effluent colloid concentrations C/C_0 (C and C_0 are effluent and influent colloid concentrations, respectively) are plotted as a function of pore volume. In both experiments, the 1156-nm colloids were deposited in 0.3 mol L^{-1} NaCl electrolyte solutions at pH 10 in Phase 1 at primary minima according to the aforementioned theoretical calculations. In Phase 2, the columns were flushed with colloid-free solutions of the same ionic strength and pH to displace suspended colloids in pore water. The similarity of breakthrough curves for Phases 1 and 2 in Fig. 6a with that in Fig. 6b indicates a high degree of reproducibility. Upon flushing with 0.001 mol L^{-1} NaCl at pH 6.0 to 6.5 in Phase 3, a small peak was observed (see Fig. 6a), denoting that a portion of colloids was released. No peak was detected, however, when the column was flushed with 0.2 mol L^{-1} NaCl (see Fig. 6b). These experimental observations are consistent with the theoretical predictions.

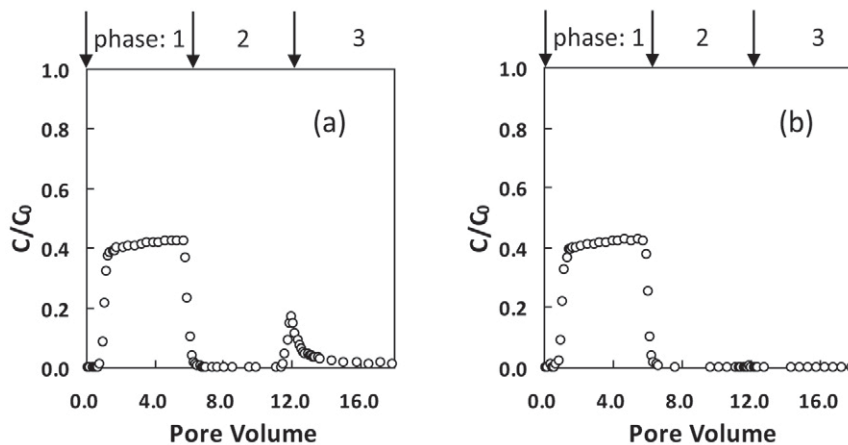


Fig. 6. Experimental breakthrough curve for 1156-nm latex particles at a concentration of 10 mg L^{-1} deposited in 0.3 mol L^{-1} NaCl in Phase 1, eluted with 0.3 mol L^{-1} NaCl in Phase 2, and then eluted in Phase 3 with (a) 0.001 mol L^{-1} NaCl or (b) 0.2 mol L^{-1} NaCl.

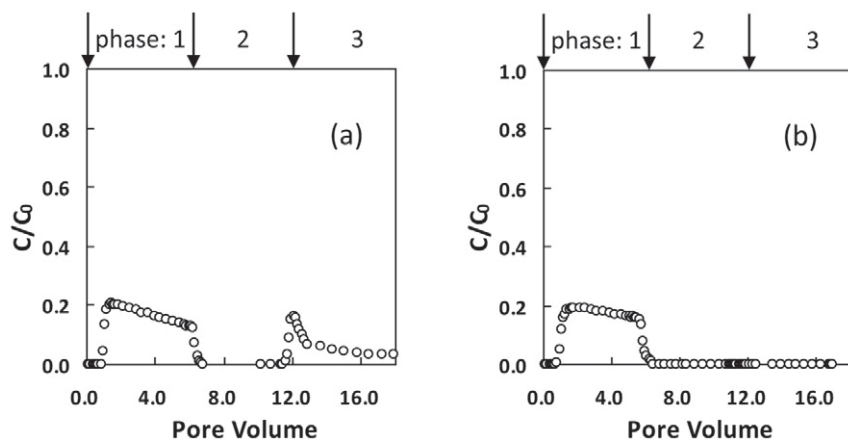


Fig. 7. Experimental breakthrough curve for 1156-nm latex particles at a concentration of 10 mg L^{-1} deposited in 0.2 mol L^{-1} CaCl_2 in Phase 1, eluted with 0.2 mol L^{-1} CaCl_2 in Phase 2, and then eluted in Phase 3 with (a) 0.001 mol L^{-1} CaCl_2 or (b) 0.1 mol L^{-1} NaCl.

Colloid breakthrough curves for the two deposition and release experiments in CaCl_2 electrolyte solutions are presented in Fig. 7. The results are very similar to those observed for the NaCl solution shown in Fig. 6 and therefore warrant similar interpretations. The breakthrough concentration was lower in the 0.2 mol L^{-1} CaCl_2 solution, however, indicating greater colloid retention than in 0.3 mol L^{-1} NaCl. In addition, the plateau values of C/C_0 decreased with time, indicating the onset of ripening, where deposited colloids acted as additional collectors. Again, the experimental observations are consistent with theoretical predictions.

It should be noted that an increase in solution pH can also detach the colloids deposited at primary minima by reversing the charges on the colloid or collector surfaces (Tufenkji and Elimelech, 2005; Ryan and Gschwend, 1994a; Chen and Elimelech, 2006; Tosco et al., 2009). It is unlikely, however, that the release of colloids in

Phase 3 was caused by surface charge reversal because this scenario was not possible in the experiments discussed above: the pH of NaCl solutions in Phases 1 and 2 (first set of experiments) was higher than that in Phase 3, and CaCl₂ had a similar pH in all three phases (second set of experiments).

Discussion

It is widely accepted that colloid deposition in secondary minima is reversible on decreasing the solution ionic strength because the decrease reduces the secondary minimum well (Litton and Olson, 1996; Redman et al., 2004; Hahn and O'Melia, 2004; Hahn et al., 2004; Tufenkji and Elimelech, 2004b, 2005; Shen et al., 2007). There is a discrepancy, however, about the reversibility of colloid deposition in primary minima on reduction of the solution ionic strength in the literature. Considerable recent studies (Hahn and O'Melia, 2004; Hahn et al., 2004; Shen et al., 2007, 2008; Torkzaban et al., 2010) believed that colloid deposition in primary minimum is irreversible when the solution ionic strength is reduced. This is because, according to DLVO theory, the depth of the primary minimum increases with decreasing ionic strength and the potential interaction energy function increases more rapidly from zero separation distance at lower ionic strength (Hahn and O'Melia, 2004; Hahn et al., 2004). The observed releases of colloids were attributed to those initially deposited in secondary minima in these studies. In contrast, earlier studies viewed the primary minimum as the only location for colloid deposition and believed that colloid deposition in the primary minimum could be reversible to accommodate the observed detachments with a decrease in ionic strength in the experiments (McDowell-Boyer, 1992; Amirtharajah and Raveendran, 1993; Nocito-Gobel and Tobiasson, 1996; Bergendahl and Grasso, 2003). However, the deposition stages of these experiments were conducted under unfavorable conditions, and it is unclear whether the released colloids originated from primary or secondary minima. Alternatively, a number of studies (Bales and Li, 1993; Ryan and Gschwend, 1994a; Roy and Dzombak, 1996; Chen and Elimelech, 2006; Tosco et al., 2009) have conducted experiments under favorable conditions to allow colloids to unambiguously deposit in primary minima and found that detachment occurred when the solution ionic strength was decreased. These observations are consistent with the theoretical and experimental results in our study, in contrast to the prediction by the classic DLVO model. Because detachment from the primary minimum is dependent on various experimental conditions (e.g., particle size, collector roughness, the amount of colloids initially deposited, and the ionic strength of the solution for release), the amount of colloids released differed significantly in those experiments.

Although our study considered only the roughness on the collector surface and assumed the colloid surface to be smooth, roughness is common on the surfaces of natural colloids (e.g., viruses and bacteria). Whereas the existence of asperities on a colloid can reduce

interaction energy barriers and facilitate deposition of colloids in primary minima (Suresh and Walz, 1996), the asperities also assist detachment by providing a finite separation between the main body of the colloid and collector surfaces. Once the solution chemistry changes, the main body of the colloid may experience a repulsive force from the collector (similar to Fig. 4b). Moreover, the coupled influence of asperities on both colloids and collectors can further enhance the detachment. Whereas surface charge heterogeneity only alters the magnitude of DLVO interaction energies and cannot change the shape of DLVO interaction energy profiles like surface roughness (e.g., the elimination of primary minima), it can act together with surface roughness and further assist with detachment.

Although the importance of surface roughness on colloid *deposition* has been broadly recognized, the influence of surface roughness on colloid *detachment* has received little attention. Only very limited studies (Das et al., 1994; Bergendahl and Grasso, 1999, 2000; Burdick et al., 2005) have examined the effects of surface roughness on the hydrodynamic detachment of colloids at primary minima by considering a specific interaction configuration, i.e., colloid aside the asperity (see Fig. 1b). They found that surface roughness inhibits colloid detachment by comparing the adhesive torque and hydrodynamic torque. These studies did not consider the interaction between the colloid and the asperity, however, and only estimated the influence of roughness on the lever arms of the hydrodynamic and adhesive torques. Our study shows that, because of the variability of local geometric configurations caused by the physical heterogeneity of collector surfaces (e.g., Supplemental Fig. S1), surface roughness can both enhance (e.g., Fig. 1a) and reduce (e.g., Fig. 1b) colloid detachment. Although we only examined the influence of surface heterogeneity on the detachment of colloids initially deposited under favorable conditions, the effect of surface heterogeneity on the detachment of colloids initially deposited under unfavorable conditions is also expected. Indeed, considerable experimental studies (Ryan and Gschwend, 1994b; Yiantsios and Karabelas, 1995; Loveland et al., 1996; Nocito-Gobel and Tobiasson, 1996; Roy and Dzombak, 1996; Bergendahl and Grasso, 2000; Canseco et al., 2009; Torkzaban et al., 2010) have shown continuous release of colloids initially deposited under both favorable and unfavorable conditions when experimental conditions (e.g., ionic strength, flow velocity, and pH) were sequentially increased or decreased. This clearly indicates that the colloids deposited at primary and secondary minima are associated with collectors with different levels of attraction, and the colloids with smaller attraction are easier to release. Microscopy examinations (Bowen and Doneva, 2000; Rabinovich et al., 2000) also verified that the adhesion forces that colloids experience at different locations of rough collector surfaces differ significantly.

The theoretical results of our study provide plausible explanations for the observed discrepancies between theoretical predictions

and experimental results for colloid detachment from primary minima. As discussed above, by including the influence of surface roughness, the discrepancy between classic DLVO model prediction and the experimental observation that the release of colloids from primary minima increases with decreasing ionic strength is resolved. Our results also demonstrate that, contrary to the detachment model prediction (Dahneke, 1975; Bergendahl and Grasso, 2003), colloid transport across an energy barrier is not the rate-limiting step for release from the energy attraction well, which is in agreement with experimental observations (Ryan and Gschwend, 1994b; Roy and Dzombak, 1996). In addition, Loveland et al. (1996) and Ryan and Gschwend (1994b) showed that to fit the DLVO model prediction with the experimental results of detachment caused by an increase in solution pH or decrease in solution ionic strength, an unusually high value (e.g., 2 nm in Ryan and Gschwend, 1994b) has to be assigned for the Born collision parameter, which controls the closest separation distance between the colloid and the collector. Surface roughness is probably the cause of the large closest separation distance between the colloid and collector surface.

Conclusions

Colloid deposition in primary minima has been traditionally considered to be irreversible when the solution ionic strength is reduced because, according to DLVO theory, the depth of the primary minimum increases with decreasing ionic strength and the potential interaction energy function increases more rapidly from zero separation distance at lower ionic strength. This conclusion was obtained, however, based on the assumption that both colloid and collector surfaces are perfectly smooth. A superposition method was used to evaluate the net interaction energy when a colloid contacts a roughness element. Theoretical calculations showed that colloids at the tip of nanoscale protruding asperities could experience a repulsive force at zero separation distance and, at low ionic strengths (e.g., 0.001 mol L^{-1} in this study), the primary minimum in the DLVO interaction energy curves could be completely eliminated by the repulsive interaction between the colloid and a reference flat surface in the presence of a roughness element. Therefore, the colloids initially deposited at these locations via primary minima association will be released following a significant reduction in the solution ionic strength. The theoretical results were in agreement with column experiment results from the present study and additional observations reported in the literature. While nanoscale asperities have been found to increase colloid deposition by decreasing the energy barrier under unfavorable conditions, our study demonstrates that these asperities also facilitate detachment of colloids initially deposited under favorable chemical conditions. Our study further suggests that the heterogeneous attractions of attached colloids to collectors must be considered in a detachment model for accurate predictions of their release behaviors in the subsurface environment.

Acknowledgments

We acknowledge the financial support provided by the National Natural Science Foundation of China (no. 40901109), Specialized Research Fund for the Doctoral Program of Higher Education (no. 20090008120041), Chinese Universities Scientific Fund (2011JJS165), Beijing Natural Science Foundation (no. 6123034), the National Research Initiative Competitive Grants no. 2006-02551 and 2008-02803 from the USDA Cooperative State Research, Education, and Extensive Services, and U.S. National Science Foundation under CBET-0932686.

References

- Amirtharajah, A., and P. Raveendran. 1993. Detachment of colloids from sediments and sand grains. *Colloids Surf. A* 73:211–227. doi:10.1016/0927-7757(93)80017-9
- Bales, R.C., and S. Li. 1993. MS-2 and poliovirus transport in porous media: Hydrophobic effects and chemical perturbations. *Water Resour. Res.* 29:957–963. doi:10.1029/92WR02986
- Bergendahl, J., and D. Grasso. 1999. Prediction of colloid detachment in a model porous media: Thermodynamics. *AIChE J.* 45:475–484. doi:10.1002/aic.690450305
- Bergendahl, J., and D. Grasso. 2000. Prediction of colloid detachment in a model porous media: Hydrodynamics. *Chem. Eng. Sci.* 55:1523–1532.
- Bergendahl, J.A., and D. Grasso. 2003. Mechanistic basis for particle detachment from granular media. *Environ. Sci. Technol.* 37:2317–2322. doi:10.1021/es0209316
- Bhattacharjee, S., C.-H. Ko, and M. Elimelech. 1998. DLVO interaction between rough surfaces. *Langmuir* 14:3365–3375. doi:10.1021/la971360b
- Bowen, W.R., and T.A. Doneva. 2000. Atomic force microscopy studies of membranes: Effect of surface roughness on double-layer interactions and particle adhesion. *J. Colloid Interface Sci.* 229:544–549. doi:10.1006/jcis.2000.6997
- Burdick, G.M., N.S. Berman, and S.P. Beaudoin. 2005. Hydrodynamic particle removal from surfaces. *Thin Solid Films* 488:116–123. doi:10.1016/j.tsf.2005.04.112
- Canseco, V., A. Djehiche, H. Bertin, and A. Omari. 2009. Deposition and re-entrainment of model colloids in saturated consolidated porous media: Experimental study. *Colloids Surf. A* 352:5–11. doi:10.1016/j.colsurfa.2009.09.033
- Chen, K.L., and M. Elimelech. 2006. Aggregation and deposition kinetics of fullerene (C60) nanoparticles. *Langmuir* 22:10994–11001. doi:10.1021/la062072v
- Cooper, K., A. Gupta, and S. Beaudoin. 2001. Simulation of the adhesion of particles to surfaces. *J. Colloid Interface Sci.* 234:284–292. doi:10.1006/jcis.2000.7276
- Dahneke, B. 1975. Kinetic theory of the escape of particles from surfaces. *J. Colloid Interface Sci.* 50:89–107. doi:10.1016/0021-9797(75)90257-X
- Das, S.K., R.S. Schechter, and M.M. Sharma. 1994. The role of surface roughness and contact deformation on the hydrodynamic detachment of particles from surfaces. *J. Colloid Interface Sci.* 164:63–77. doi:10.1006/jcis.1994.1144
- Elimelech, M., and C.R. O'Melia. 1990a. Kinetics of deposition of colloidal particles in porous media. *Environ. Sci. Technol.* 24:1528–1536. doi:10.1021/es00080a012
- Elimelech, M., and C.R. O'Melia. 1990b. Effect of particle size on collision efficiency in the deposition of Brownian particles with electrostatic energy barriers. *Langmuir* 6:1153–1163. doi:10.1021/la00096a023
- Feke, D.L., N.D. Prabhu, J.A. Mann, Jr. and J.A. Mann III. 1984. A formulation of the short-range repulsion between spherical colloidal particles. *J. Phys. Chem.* 88:5735–5739. doi:10.1021/j150667a055
- Hahn, M.W., D. Abadizic, and C.R. O'Melia. 2004. Aquasols: On the role of secondary minima. *Environ. Sci. Technol.* 38:5919–5924.
- Hahn, M.W., and C.R. O'Melia. 2004. Deposition and reentrainment of Brownian particles in porous media under unfavorable chemical conditions: Some concepts and applications. *Environ. Sci. Technol.* 38:210–220. doi:10.1021/es030416n
- Ho, N.F.H., and W.I. Higuchi. 1968. Preferential aggregation and coalescence in heterodispersed systems. *J. Pharm. Sci.* 57:436–442. doi:10.1002/jps.2600570314
- Hoek, E.M.V., and G.K. Agarwal. 2006. Extended DLVO interactions between spherical particles and rough surfaces. *J. Colloid Interface Sci.* 298:50–58. doi:10.1016/j.jcis.2005.12.031
- Hoek, E.M.V., S. Bhattacharjee, and M. Elimelech. 2003. Effect of membrane surface roughness on colloid–membrane DLVO interactions. *Langmuir* 19:4836–4847. doi:10.1021/la027083c
- Hogg, R., T.W. Healy, and D.W. Fuerstenau. 1966. Mutual coagulation of colloidal dispersions. *Trans. Faraday Soc.* 62:1638–1651. doi:10.1039/tf9666201638
- Huang, X., S. Bhattacharjee, and E.M.V. Hoek. 2010. Is surface roughness a “scapegoat” or a primary factor when defining particle–substrate interactions? *Langmuir* 26:2528–2537. doi:10.1021/la9028113

- Jaiswal, R.P., G. Kumar, C.M. Kilroy, and S.P. Beaudoin. 2009. Modeling and validation of the van der Waals force during the adhesion of nanoscale objects to rough surfaces: A detailed description. *Langmuir* 25:10612–10623. doi:10.1021/la804275m
- Katainen, J., M. Paajanen, E. Ahtola, V. Pore, and J. Lahtinen. 2006. Adhesion as an interplay between particle size and surface roughness. *J. Colloid Interface Sci.* 304:524–529. doi:10.1016/j.jcis.2006.09.015
- Kemps, J.A.L., and S. Bhattacharjee. 2009. Particle tracking model for colloid transport near planar surfaces covered with spherical asperities. *Langmuir* 25:6887–6897. doi:10.1021/la9001835
- Litton, G.M., and T.M. Olson. 1996. Particle size effects on colloid deposition kinetics: Evidence of secondary minimum deposition. *Colloids Surf. A* 107:273–283. doi:10.1016/0927-7757(95)03343-2
- Loveland, J.P., J.N. Ryan, G.L. Amy, and R.W. Harvey. 1996. The reversibility of virus attachment to mineral surfaces. *Colloids Surf. A* 107:205–221. doi:10.1016/0927-7757(95)03373-4
- Ma, H., J. Pedel, P. Fife, and W. Johnson. 2009. Hemispheres-in-cell geometry to predict colloid deposition in porous media. *Environ. Sci. Technol.* 43:8573–8579. doi:10.1021/es901242b
- McDowell-Boyer, L.M. 1992. Chemical mobilization of micron-sized particles in saturated porous media under steady flow conditions. *Environ. Sci. Technol.* 26:586–593. doi:10.1021/es00027a023
- Nocito-Gobel, J., and J.E. Tobiason. 1996. Effects of ionic strength on colloid deposition and release. *Colloids Surf. A* 107:223–231. doi:10.1016/0927-7757(95)03340-8
- Rabinovich, Y.I., J.J. Adler, A. Ata, R.K. Singh, and B.M. Moudgil. 2000. Adhesion between nanoscale rough surfaces: II. Measurement and comparison with theory. *J. Colloid Interface Sci.* 232:17–24. doi:10.1006/jcis.2000.7168
- Rajagopalan, R., and C. Tien. 1976. Trajectory analysis of deep-bed filtration with the sphere-in-cell porous media model. *AIChE J.* 22:523–533. doi:10.1002/aic.690220316
- Redman, J.A., S.L. Walker, and M. Elimelech. 2004. Bacterial adhesion and transport in porous media: Role of the secondary energy minimum. *Environ. Sci. Technol.* 38:1777–1785. doi:10.1021/es034887l
- Roy, S.B., and D.A. Dzombak. 1996. Na⁺–Ca²⁺ exchange effects in the detachment of latex colloids deposited in glass bead porous media. *Colloids Surf. A* 119:133–139. doi:10.1016/S0927-7757(96)03764-8
- Ruckenstein, E., and D.C. Prieve. 1976. Adsorption and desorption of particles and their chromatographic separation. *AIChE J.* 22:276–283. doi:10.1002/aic.690220209
- Ryan, J.N., and M. Elimelech. 1996. Colloid mobilization and transport in groundwater. *Colloids Surf. A* 107:1–56. doi:10.1016/0927-7757(95)03384-X
- Ryan, J.N., and P.M. Gschwend. 1994a. Effect of solution chemistry on clay colloid release from an iron oxide-coated aquifer sand. *Environ. Sci. Technol.* 28:1717–1726. doi:10.1021/es00058a025
- Ryan, J.N., and P.M. Gschwend. 1994b. Effect of ionic strength and flow rate on colloid release: Relating kinetics to intersurface potential energy. *J. Colloid Interface Sci.* 164:21–34. doi:10.1006/jcis.1994.1139
- Saiers, J.E., and J.N. Ryan. 2005. Colloid deposition on non-ideal porous media: The influences of collector shape and roughness on the single-collector efficiency. *Geophys. Res. Lett.* 32:L21406. doi:10.1029/2005GL024343
- Shang, J., C. Liu, Z. Wang, H. Wu, K. Zhu, J. Li, and J. Liu. 2010. In-situ measurements of engineered nanoporous particle transport in saturated porous media. *Environ. Sci. Technol.* 44:8190–8195. doi:10.1021/es1015586
- Shen, C., Y. Huang, B. Li, and Y. Jin. 2008. Effects of solution chemistry on straining of colloids in porous media under unfavorable conditions. *Water Resour. Res.* 44:W05419. doi:10.1029/2007WR006580
- Shen, C., Y. Huang, B. Li, and Y. Jin. 2010. Predicting attachment efficiency of colloid deposition under unfavorable attachment conditions. *Water Resour. Res.* 46:W11526. doi:10.1029/2010WR009218
- Shen, C., B. Li, Y. Huang, and Y. Jin. 2007. Kinetics of coupled primary- and secondary-minimum deposition of colloids under unfavorable chemical conditions. *Environ. Sci. Technol.* 41:6976–6982. doi:10.1021/es070210c
- Shen, C., B. Li, C. Wang, Y. Huang, and Y. Jin. 2011. Surface roughness effect on deposition of nano- and micro-sized colloids in saturated columns at different solution ionic strengths. *Vadose Zone J.* 10:1071–1081. doi:10.2136/vzj2011.0011
- Suresh, L., and J.Y. Walz. 1996. Effect of surface roughness on the interaction energy between a colloidal sphere and a flat plate. *J. Colloid Interface Sci.* 183:199–213. doi:10.1006/jcis.1996.0535
- Suresh, L., and J.Y. Walz. 1997. Direct measurement of the effect of surface roughness on the colloidal forces between a particle and flat plate. *J. Colloid Interface Sci.* 196:177–190. doi:10.1006/jcis.1997.5216
- Torkzaban, S., H.N. Kim, J. Šimůnek, and S.A. Bradford. 2010. Hysteresis of colloid retention and release in saturated porous media during transients in solution chemistry. *Environ. Sci. Technol.* 44:1662–1669. doi:10.1021/es903277p
- Tosco, T., A. Tiraferri, and R. Sethi. 2009. Ionic strength dependent transport of microparticles in saturated porous media: Modeling mobilization and immobilization phenomena under transient chemical conditions. *Environ. Sci. Technol.* 43:4425–4431. doi:10.1021/es900245d
- Tufenkji, N., and M. Elimelech. 2004a. Correlation equation for predicting single-collector efficiency in physicochemical filtration in saturated porous media. *Environ. Sci. Technol.* 38:529–536. doi:10.1021/es034049r
- Tufenkji, N., and M. Elimelech. 2004b. Deviation from the classical colloid filtration theory in the presence of repulsive DLVO interactions. *Langmuir* 20:10818–10828. doi:10.1021/la0486638
- Tufenkji, N., and M. Elimelech. 2005. Breakdown of colloid filtration theory: Role of the secondary energy minimum and surface charge heterogeneities. *Langmuir* 21:841–852. doi:10.1021/la048102g
- Yao, K.M., M.T. Habibian, and C.R. O'Melia. 1971. Water and wastewater filtration: Concepts and applications. *Environ. Sci. Technol.* 5:1105–1112. doi:10.1021/es60058a005
- Yiantsios, S.G., and A.J. Karabelas. 1995. Detachment of spherical microparticles adhering on flat surfaces by hydrodynamic forces. *J. Colloid Interface Sci.* 176:74–85. doi:10.1006/jcis.1995.0009
- Zhuang, J., J. Qi, and Y. Jin. 2005. Retention and transport of amphiphilic colloids under unsaturated flow conditions: Effect of particle size and surface property. *Environ. Sci. Technol.* 39:7853–7859. doi:10.1021/es050265j